Nat Hazards (2012) 60:241–261
DOI 10.1007/s11069-011-0007-2

ORIGINAL PAPER

Vulnerability of buildings to debris flow impact

M. Jakob · D. Stein · M. Ulmi

Received: 26 July 2011 / Accepted: 11 October 2011 / Published online: 21 October 2011

Abstract Quantitative risk assessments (QRAs) for landslide hazards are increasingly being executed to determine an unmitigated level of risk and compare it with risk tolerance criteria set by the local or federal jurisdiction. This approach allows urban planning with a scientific underpinning and provides the tools for emergency preparedness. Debris-flow QRAs require estimates of the hazard probability, spatial and temporal probability of impact (hazard assessment) and vulnerability of the elements at risk. The vulnerability term is perhaps the most difficult to estimate confidently because (a) human death in debris flows is most commonly associated with building damage or collapse and is thus an indirect consequence and (b) the type and scale of building damage is very difficult to predict. To determine building damage, an intensity index (I_{DF}) was created as the product of maximum expected flow depth d and the square of the maximum flow velocity v ($I_{DF} = dv^2$). The I_{DF} surrogates impact force and thus correlates with building damage. Four classes of building damage were considered ranging from nuisance flood/sedimentation damage to complete destruction. Sixty-six well-documented case studies in which damage, flow depth and flow velocity were recorded or could be estimated were selected through a search of the global literature, and I_{DF} was plotted on a log scale against the associated damage. As expected, the individual damage classes overlap but are distinctly different in their respective distributions and group centroids. To apply this vulnerability model, flow velocity and flow depth need to be estimated for a given building location and I_{DF} calculated. Using the existing database, a damage probability (P_{DF}) can then be computed. P_{DF} can be applied directly to estimate the likely insurance loss or associated loss of life. The model presented here should be updated with more case studies and is therefore made openly available to international researchers who can access it at http://chis.nrcan.gc.ca/QRA-EQR/index-eng.php.

M. Jakob (✉) · D. Stein
BGC Engineering Inc., 500-1045 Howe Street, Vancouver, BC V6Z 2A9, Canada
e-mail: mjakob@bgcengineering.ca

D. Stein
e-mail: dstein@bgcengineering.ca

M. Ulmi
Geological Survey of Canada, 625 Robson Street, Vancouver, BC V6B 5J3, Canada

Keywords Debris flow · Vulnerability · Quantitative risk assessments · Hazard assessments · HAZUS · Damage functions · Landslides

1 Introduction

In recent years, there has been a global trend away from hazard-based assessments of geohazards and towards a risk-based approach. The former uses a design return period which may either be arbitrarily set or associated with return periods used for other geohazards such as earthquakes or floods. Risk assessments in which numerical analyses are used are termed quantitative risk assessments, and these require specific input parameters. For debris flows, risk is commonly expressed as risk of loss of life or economic risk. Other indirect debris-flow consequences such as environmental losses, corporate reputation loss or intangibles such as human suffering are sometimes mentioned anecdotally but are not quantified routinely.

For economic or loss of life risk, similar input parameters are required. For loss of life risk, the risk (R_{DF}) equation is:

$$R_{DF} = P_H \times P_{S:H} \times P_{T:S} \times V \times E \quad (1)$$

where P_H is the annual probability of the landslide occurring; $P_{S:H}$ is the spatial probability that the landslide will reach the individual most at risk; $P_{T:S}$ is the temporal probability that the individual most at risk will be present when the landslide occurs; V is the vulnerability, or probability of loss of life if the individual is impacted; and E is the number of people at risk, which is equal to 1 for the determination of individual risk.

P_H can be estimated through the application of a number of absolute dating methods suitable for the environment in question. P_H is expressed as the annual probability of occurrence. $P_{S:H}$ is typically estimated through detailed mapping of past flows, empirical or numerical analysis or a combination. $P_{T:S}$ can be estimated through surveys or broad assumptions that are typically reasonably accurate for full-time dwellings but need to be adjusted, for example, for recreational properties. V is perhaps the least understood variable because of lack of consistent data and the problem of predicting damage to a building for a set of debris flow intensity variables. V can be expressed either as the projected monetary loss to a building or infrastructure, or as a probability of life loss between zero and 1. This paper addresses the vulnerability to buildings even though it is realized that building damage is closely related to injury and death.

Previous work has identified the need for a better understanding of vulnerability for debris flow impacts to buildings. For example, Fuchs et al. (2007) used an intensively studied debris flow event in the Austrian Alps to derive a quantitative vulnerability function for buildings affected by the debris flow. Vulnerability was defined as the quotient between the loss of the individual reinstatement value for each element at risk and against debris-flow intensity expressed as deposit height. A polynomial function was fitted with a correlation coefficient of 0.86. Significant variability in vulnerabilities was found for deposit thicknesses in excess of 1.5 m. Comparisons with work by Borter (1999) and Fell and Hartford (1997) showed that the values presented by Fuchs et al. (2007) yielded significantly lower vulnerabilities for deposit depths in excess of 1 m. In the case of Fell and Hartford (1997), the higher vulnerability estimates may be associated with the light timber frame construction techniques that provide less strength to debris-flow impact than the brick masonry and concrete construction as encountered in the Fuchs et al.'s (2007)

example. Furthermore, a strong dependency on vulnerability was found if debris was able to enter a building and destroy its contents.

The work by Fuchs et al. (2007) is valuable as it is the first detailed site-specific analysis of loss potential for a variable that can easily be measured in the field. Limitations are introduced by neglecting flow velocity due to the difficulty in back-calculating it for the buildings used in their analysis (Fuchs, personal communication, 2011). As shown in the following section, flow velocity is a key variable in estimating impact forces that translate into building vulnerability. Another point of criticism is that the results offered by Fuchs et al. (2007) are not transferable to other construction types as pointed out by the authors. Finally, in many jurisdictions, landslide damage is not insurable, insured losses are unknown and, therefore, a damage ratio as used by Fuchs et al. (2007) as a surrogate variable for debris-flow vulnerability cannot be constructed.

Totschnig et al. (2011) elaborated on the earlier work by Fuchs and used data from three well-documented debris flow events in the Austrian Alps to quantify vulnerability for residential buildings. Totschnig et al. (2011) used a damage ratio ($I_R = I/H$) with I being the deposition height and H the height of the affected building. This damage ratio was used as a surrogate for vulnerability to characterize the damage potential of a building. The authors calculated the reconstruction value of each building based on an average insured cost per square metre. A complex equation was formulated to determine a building's value based on building area, number of stories, unit price and a reduction factor for the state of maintenance. Loss data were obtained from the respective administrative offices. To quantify process intensity, the authors followed the approach by Fuchs et al. (2007) based on relative intensity I_R. Totschnig et al. (2011) realized that impact pressures are relevant but pointed out that only deposition height and flow depths are regularly documented for debris flows in Austria. The authors used data on 67 residential buildings with a total damage of € 5.5 million with vulnerability ranges from 0.001 to 1.0 and a mean of 0.17. A modified Frechet distribution was applied to fit the relative intensity to damage in relation to building height.

Fuchs et al.'s (2007) and Totschnig et al.'s (2011) approaches appear well suited for areas where loss potential can be quantified, for example, by using insurance loss functions. In most countries, however, a reasonable estimate of the damage in terms of cost is not possible because of the lack of data on reconstruction costs or building value. For those areas, a simpler approach may be more suitable which relates debris flow intensity to classes of building damage, which in turn can be associated with an insured loss. Monetary losses can be calculated directly from the assumed insured losses reported in this paper or be calculated for specific building locations based on asset inventories and replacement costs developed by HAZUS (HAZards in the United States), a geographic information system-based natural hazard loss estimation software package developed by the Federal Emergency Management Agency (FEMA).

Another approach to describe structure vulnerability to debris flow activity is described by Haugen and Kaynia (2008) who examined how vibratory motion from earthquakes can be used to predict damage induced from debris flows. Haugen's and Kaynia's (2008) theory states that ground vibrations from an earthquake will damage a given structure in the same way as vibratory forces from debris flow impact. Accepting this assumption would allow the use of a large body of literature on earthquake vibration on structures and apply the fragility curves developed for earthquakes in the HAZUS program and transfer those to debris flows. The fragility curves are developed for each structure from Model Building Types (FEMA 2003, p. 176) and ratios involving building height. (FEMA 2003, p. 208) The input for the fragility curve is spectral displacement which corresponds to the

maximum displacement during an earthquake. The debris flow equivalent spectral displacement can be calculated from the sum of the hydrostatic spectral displacement and the dynamic spectral displacement. To calculate the spectral displacements, debris flow velocity and flow depth are required. The output of the fragility curve is a probability of damage. This model was compared against the 1998 Sarno (Italy) debris flows and was found to accurately predict building damage 5 out of 6 times.

Haugen and Kaynia's model requires a categorization of the building types into 37 different groups and knowledge of building heights. It is unclear whether vibratory motion triggered by earthquakes can be compared to and applied in a predictive model to the impact forces by debris flows. This would need to be tested empirically or through field tests. Furthermore, multiple surge waves can generate repetitive loads but are not accounted for in the model by Haugen and Kaynia. The model has been applied only to one case study, and the robustness of the model would need to be tested on a larger variety of cases.

2 Methods

In most instances, data on actual and insured losses were unavailable, which precluded an analysis similar to that conducted by Fuchs et al. (2007). Furthermore, insured losses are not necessarily an exact representation of the actual losses and, as pointed out by Fuchs et al. (2007), hinge on the specific actuarial and economic conditions of the region to which the vulnerability index is applied. In addition, HAZUS provides asset inventory with specific building values and replacement costs that allow the estimation of monetary losses due to debris flow impacts. Thus, in our work, we focused on a more generalized approach.

Vulnerability was defined as the qualitative damage to a building as ranked in four damage classes, from some sedimentation, some structural damage, major structural damage, to complete building destruction (Table 1). The primary objective was to find a simple function that would allow a prediction of likely losses that can then be integrated into the HAZUS program, allowing it to be extended from floods to debris flows. A probabilistic assessment of damage was sought, rather than a single damage figure. Such work can supplement expert judgment that is typically applied to estimate building vulnerability.

A database of 68 events has been populated from a review of journals and conference proceedings (Table 2). Debris flow events ranging from Class 1 to Class 7 (Jakob 2005) were entered resulting in a spectrum of events ranging from those large enough to destroy entire villages (Fig. 1) to those just large enough to cause some sedimentation in a home's basement (Fig. 2). For each event, the key information extracted or estimated was flow

Table 1 Damage classes and definitions for impacts to residential buildings

Damage class	Damage description
Some sedimentation (I)	Sediment-laden water ingresses building's main floor or basement; requires renovation; up to 25% insured loss
Some structural damage (II)	Some supporting elements damaged and could be repaired with major effort; 25–75% insured loss
Major structural damage (III)	Damage to crucial building-supporting piles, pillars and walls will likely require complete building reconstruction; >75% insured loss
Complete destruction (IV)	Structure is completely destroyed and/or physically transported from original location; 100% insured loss

depth at the point of impact (d), velocity at the point of impact (v), peak discharge (Q), total volume of material involved (V) and the extent of damage to a given structure (D). Where available, data were gathered on the type of destruction, as well as maximum boulder size, type of structure affected and impact on the affected population.

A variety of impact vulnerability indices were considered including v, d, v^2d and vd^2. Each index was plotted against the observed damage class. As expected, v^2d showed the most consistent relationship to building damage and was thus adopted as the most representative index. This index is meaningful from a kinematic point of view because flow depth and flow velocity are key input variables in determining the dynamic forces exerted by debris flows. In classical mechanics, the kinetic energy (E_k) of a non-rotating rigid body is:

$$E_k = 0.5\, mv^2 \tag{2}$$

with m being the mass.

Kherkheulidze (1976) suggests a mean debris-flow impact pressure with a static and dynamic component (Eq. 3):

$$p = 0.1\, \rho_d g\left(5h + v^2\right) \tag{3}$$

where p is the mean pressure in kN/m^2, ρ_d is the debris flow density in kg/m^3, g is the acceleration of gravity (m/s^2), h is the flow depth and v the flow velocity.

Armanini (1997) combined experiments and theory and derived a force P_{df} as per Eq. 4:

$$P_{df} = 4.5\rho_d g h^2. \tag{4}$$

Hübl and Holzinger (2003) derived a debris-flow maximum impact pressures (P_{max}) based on laboratory experiments. For Froude numbers between 1 and 15, the authors suggest:

$$P_{max} = 4.5\rho_d v^{0.8}(gh)^{0.6}. \tag{5}$$

Hungr et al. (1984) suggest a force per unit width for a perpendicular impact as:

$$P = (X_L)v^2 \tag{6}$$

where X_L is total runout distance. Hungr et al. (1984) also recommend the use of the momentum equation (Eq. 7) to determine dynamic thrust loading.

$$F = \rho_d A v^2 \sin\beta \tag{7}$$

where F is the total thrust force, A is the flow cross-section area and β is the least angle between the face of the barrier and flow direction. In this case, the debris-flow surge is considered a single flow prism travelling with a uniform velocity equal to the mean velocity. Hungr et al. (1984) further recommend that the load calculated with Eq. 7 be distributed over an area equal to the expected debris flow width and approximately 1.5 m greater in height to account for the forming of a stagnant wedge in front of the barrier's toe.

The above equations re-emphasize the strong dependency of impact force on flow velocity which is embedded in hydraulic theory.

3 Results

Based on our compilation, we were able to total the number of events per damage class (Table 3) and construct a probability matrix (Table 4) that estimates the expected damage

Table 2 Database and references used for damage probability function

Creek name	Event date	D*** (m)	v(m/s)# (min)	v(m/s)# (max)	I_{DF}** (min)	I_{DF}** (max)	I_{DF}** (avg)	Structure type	Impact damage	References
Hummingbird Creek, Canada	11-07-1997	4	5	7	100	196	148	Greenhouse	Major structural	Jakob et al. (2000)
		2*	3*	5*	18	50	34	Wood frame	Major structural	
		1.5		2		6	6	Highway	Some structural	
Aa River, China	30-07-2000	4	5	10	100	400	250	Village (130 homes)	Complete	Suwa (2003)
Dora Baltea River, Italy	15-10-2000	7	7	11	343	847	595	2 Houses	Complete	Tropeano et al. (2003)
Gully near San-Jy, Tapei	26-10-1998	1.5	7	11	73.5	181.5	127.5	2 storey building	Complete	Chou et al. (2000)
Harihara River, Japan	10-07-1997	1.5*	9*	10*	121.5	150	135	18 wooden homes	Major structural	Nakagawa et al. (2000)
Gamaharazawa Gully, Japan	6-12-1996	2*	5*	11*	50	242	146	Construction Site	Some structural	Suwa and Yamakoshi (2000)
Flank Collapse at Casita Volcano, Nicaragua	30-10-1998	5	23	28	2,645	3,920	3,282	Village of El Porvenir and Rolando Rodriguez	Complete	Scott (2000)
Sarno Debris Flow 7, Italy	5-05-1998	1*	0.5	1	0.3	1	0.6	16 Masonry	Some sedimentation	Aleotti and Polloni (2003)
		1*	0.5	1	0.3	1	0.6	7 Masonry	Some structural	
		2*	1	2	2	8	5	22 Masonry	Major structural	Zanchetta et al. (2004)
Sarno Debris Flow 8, Italy	5-05-1998	1*	0.5	1	0.3	1	0.6	30 Masonry	Some sedimentation	Toyos et al. (2003)
		1*	0.5	1	0.3	1	0.6	32 Masonry	Some structural	
		2*	1	2	2	8	5	15 Masonry	Some structural	
		2*	1	2	2	8	5	10 Masonry	Major structural	
		2.1*	2	3	8	19	14	3 Masonry	Some structural	
		2.1*	2	3	8	19	14	7 Masonry	Major structural	
		2.1*	3	4	19	34	26	5 Masonry	Major structural	
		2.1*	4	5	34	53	43	1 Masonry	Major structural	

Table 2 continued

Creek name	Event date	D*** (m)	v(m/s)# (min)	v(m/s)# (max)	I_{DF}** (min)	I_{DF}** (max)	I_{DF}** (avg)	Structure type	Impact damage	References
Jou Torrent at La Guingueta, Spain	7-11-1982	1	1	2.5	1	6	4	Several homes	Some structural	Medina et al. (2008)
Shuikazi Valley, China	11-07-2003	7*	7	8	343	448	396	10 houses	Complete	Chen et al. (2005)
Britannia Beach, Canada	28-10-1921	2	2	4	8	32	20	50 homes	Complete	BGC Engineering Inc (2010)
Testalinden Creek, Canada	13-06-10	1.2	1.1	2.7	1.5	8.8	5.1	5 Residential homes	Complete	BGC Engineering Inc (2010)
Testalinden Creek, Canada	13-06-2010	1.2	1.1	2.7	1.5	8.8	5.1	2 Residential homes	Major structural	
Eng Creek, Canada	16-10-2003	0.5	5*	7*	13	24	18	Residential home	Some structural	BGC Engineering Inc (2003)
	17-10-2003	0.2	5*	7*	4	7	6	Small workshop	Some sedimentation	
	16-10-2003	0.5	3*	5*	4	12	8	Residential home	Some sedimentation	
	17-10-2003	0.5	3*	5*	4	12	8	Residential home	Some sedimentation	
Field Creek, Canada	17-10-2003	0.3	1*	2*	0.25	1	0.6	Residential home	Some sedimentation	
Dale Creek, Canada	17-10-2003	0.1	1*	2*	0.1	0.4	0.3	Residential home	Some sedimentation	
Fly by Wire Gully, Paekakariki, New Zealand	3-10-2003	1	0.1*	0.3*	0.01	0.06	0.04	Concrete motel	Some structural	Hancox (2003)
	3-10-2003	0.3	0.1*	0.3*	0.003	0.016	0.009	BP Service Station	Some sedimentation	
St. Bernard, Philippines	17-02-2006	4	20*	30*	1,600	3,600	2,600	Guinsaugon village	Complete	Catane et al. (2007)
Kuskonook Creek, Canada	7-08-2004	2	3	5	18	50	34	2 homes, heritage building, water supply station	Major structural	VanDine et al. (2005)
		1	2	3	4	9	7	Few other buildings	Some structural	
	12-09-2004	0.3	1	2	0.3	1	0.6		Some sedimentation	

Table 2 continued

Creek name	Event date	D*** (m)	v(m/s)# (min)	v(m/s)# (max)	I_{DF}** (min)	I_{DF}** (max)	I_{DF}** (avg)	Structure type	Impact damage	References
Zymoetz River, Canada	8-06-2002	2*	10	20	200	800	500	Pipeline	Complete	McDougall et al. (2006)
M Creek, Howe Sound, Canada	28-10-1981	3	4	5	48	75	62	Residence	Complete	Thurber Consultants Ltd. (1983) Blais-Stevens and Septer (2008)
Charles Creek, Howe Sound, Canada	1981	2.0	0.5	3	0.38	13.5	7	Residence	Some structural	Thurber Consultants Ltd. (1983), Blais-Stevens and Septer (2008)
Alberta Creek, Howe Sound, Canada	11-02-1983	3.5	7	9	171	283	227	3 Residences	Major structural	Thurber Consultants Ltd. (1983) Blais-Stevens and Septer (2008)
		1.5	1	4	2	24	13	1 Residence	Some structural	
Cervinara, Italy	12-1999	0.5	5	8	12.5	32	22.3	Buildings	Some structural	Revellino et al. (2004)
Uria, Venezuela	12-1999	3*	10*	15*	300	675	488	Many buildings in Uria	Complete	Garcia-Martinez and Lopez (2005)
Sorenberg, Switzerland	05-1999	0.5*	1	2	0.5	2	1.3	Residences	Some sedimentation	Zimmermann (2005)
Waterfall Creek, New Zealand	01-1994	7	13	17	1,183	2,023	1,603	Bridge	Complete	McSaveney and Davies (2005)
Newman Creek, Canada	18-11-1969	1*	1*	3*	1	9	5	House	Some structural	Blais-Stevens and Septer (2008)
Shum Wan Road Landslide, Hong Kong	13-08-1995	1	1*	7*	1	49	25	Factory	Some structural	Chen and Lee (2007)
Fei Tsui Landslide, Hong Kong	13-08-1995	1	0.5	1	0.25	1	0.63	Church	Some sedimentation	

Table 2 continued

Creek name	Event date	D*** (m)	v(m/s)# (min)	v(m/s)# (max)	I_{DF}** (min)	I_{DF}** (max)	I_{DF}** (avg)	Structure type	Impact damage	References
Berkeley Slide, North Vancouver, Canada	19-01-2005	2	9	11	162	242	202	Residence	Complete	Beaupre (2009)
		0.6	1*	2*	0.6	2.4	1.5	Residence	Some structural	
Two Mile Creek, Canada	01-1984	3*	10*	15*	300	675	488	Bridge	Complete	Bovis and Dagg (1992)
Riale Buffaga catchment, Switzerland	28-08-1997	1.5	2*	5*	6	38	22	Numerous residences	Some structural	Conedera et al. (2003)
Dry Mountain, Utah Valley, Tributary 4, US	12-11-2002	1	1*	3*	1*	9	5	Residences	Some structural	Utah Geological Survey (2002)
Nevado Del Ruiz, Mudflow, Columbia	13-11-1985	4*	1*	3*	4	36	20	Town of Armero	Complete	Rapp et al. (1991)
Wulong, Chongqing, China	5-06-2009	3*	10*	20*	300	1,200	750	12 houses and iron mine tunnel	Complete	Xu et al. (2010)
Haulien A124, Taiwan	28-07-2008	2.8*	1*	2*	3	11	7	Bridge foundation	Some structural	Hsu et al. (2010)
Haulien A072, Taiwan		1.8*	1.5*	2.5*	4.	11	7.7	Residences (rural shacks)	Major structural	
Glyssibach, Switzerland	23-08-2005	4*	6	10	144	400	272	Village of Brienz	Major structural	Mueller and Loew (2009)
Chuni Town, China	30-06-2005	1.5	3	6	14	54	34	17 poorly built homes	Complete	Ni et al. (2010)
Hailuogou, China	11-08-2005	10*	8	13	640	1,690	1,165	Electrical Station	Complete	
Kazbek Massif, Russia	20-09-2002	35*	20*	30*	14,000	31,500	22,750	Residences, 3 storey bath building, etc.	Complete	Haeberli et al. (2004)
Qiongshan Ravine, China	11-07-2003	4*	4*	8.5*	64	289	177	Residential area	Major structural	Kong et al. (2006) Chen et al. (2005)

Table 2 continued

Creek name	Event date	D*** (m)	v(m/s)# (min)	v(m/s)# (max)	I_{DF}** (min)	I_{DF}** (max)	I_{DF}** (avg)	Structure type	Impact damage	References
Nevado Huascaran, Peru	10-01-1962	3*	8*	12*	192	432	312	Large part of village of Ranrahirca	Complete	Evans et al. (2009)
	31-05-1970	4*	12*	35*	576	4,900	2,738	Many villages	Complete	
Hogawachi, Japan	19-07-2003	1	3	6	8	36	22	14 Residential homes	Major structural	Wang et al. (2008)
Miyagawa, Japan	29-09-2004	4*	5*	10*	100	400	250	Residential community	Complete	Suwa and Nakaya (2007)
Southern Leyte, Phillipines	17-02-2006	4*	10*	20*	400	1,600	1,000	Residential	Complete	Suwa and Nakaya (2007)

* Value estimated from picture or inferred from description of debris flow

** Debris flow intensity index (flow depth * flow velocity at impact)

*** Flow depth

Flow velocity

Fig. 1 Carabella, Venezuela debris flow, 1999. Damage class IV: complete destruction. The estimated I_{DF} for this event was 500. Photograph from Matthew C. Larsen, U.S. Geological Survey

Fig. 2 Damage class I: some sedimentation for a debris flow in Hatzik Valley, southwestern B.C. The estimated I_{DF} for this event is <1. Photograph: Matthias Jakob. November 2002

a given structure will suffer given an estimated debris flow intensity index (I_{DF}). These data are graphically represented in Fig. 3 with I_{DF} against damage class, histograms illustrating the number of events per case, and where available, structure type is indicated

Table 3 Impact index (I_{DF}) damage matrix showing the four construction classes, the debris flow intensity index on a log scale and the presumed insured losses

Damage class	Number of cases					Insured loss (%)
Complete destruction (IV)	0	1	4	12	6	100
Major structural damage (III)	0	4	6	5	0	>75
Some structural damage (II)	3	9	6	1	0	25–75
Some sedimentation (I)	7	4	0	0	0	<25
I_{DF}	0–1	$1–10^1$	$10^1–10^2$	$10^2–10^3$	$>10^3$	

The centre of the matrix contains the number of cases that have been included in the analysis

Table 4 Damage class probabilities

Damage class probabilities given I_{DF} (%) ALL DATA					
Complete destruction (IV)	0	6	25	67	100
Major structural damage (III)	0	22	38	28	0
Some structural damage (II)	30	50	37	5	0
Some sedimentation (I)	70	22	0	0	0
I_{DF}	0–1	$1–10^1$	$10^1–10^2$	$10^2–10^3$	$>10^3$

The percentage numbers in the table indicate the likelihood of damage occurring for a given I_{DF}. For example, for a I_{DF} between 100 and 1,000, there is a 67% likelihood that it will result in complete destruction and a 28% likelihood that major structural damage will occur. It is unlikely (5%) that some structural damage occurs

by unique symbols. To apply this matrix, flow velocities and maximum flow depth need to be estimated. Velocities can be calculated, for example, through runup on buildings using Chow's (1959) formula ($v = 2\ g\Delta h)^{0.5}$ or Wigmosta (1983), ($v = 1.2\ g\Delta h)^{0.5}$ where Δh is the runup height. Alternative velocity estimates can be back-calculated using the forced-vortex equation ($v = gr_c\cos\Theta\tan\alpha)^{0.5}$ (Chow 1959) where r_c is the radius of curvature to the centre of mass and α being the superelevation angle. In the absence of runup and superelevation observations, channel parameters can be used to back-calculate velocities as suggested by Hungr et al. (1984) with $v = (\gamma S/K\mu)h^2$ where γ is the unit weight, μ is the dynamic viscosity of the flow, S is the channel slope, K is a shape factor and h is the flow thickness, or by Rickenmann (1999) with $v = 2.1Q^{0.33}S^{0.33}$ where Q is the peak discharge. Numerical modelling can also be used to estimate flow velocities but will require calibration to render reasonable results.

Flow depths can be determined empirically using test trenches that show deposition depths of past flows in the area of interest, which may need to be increased by a nominal amount to account for water dissipation and settlement after flow ceases. Numerical models also provide estimates of flow depth but require calibration with flows of known depth.

As with all risk assessments, differentiation is required for a variety of return period scenarios as flow volumes, peak flows and velocities are roughly proportional to debris flow return period. A 1000-year return period flow will almost always have higher flow velocities and higher flow depths than a 100-year return period flow. Therefore, building vulnerability needs to be assessed for each hazard scenario considered in the risk assessment.

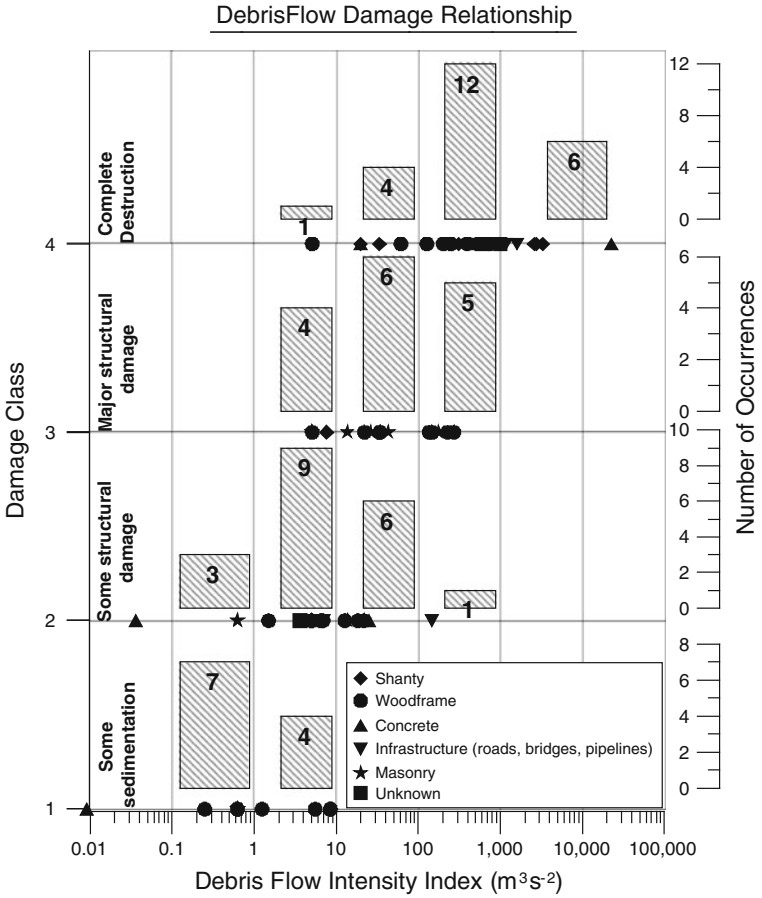

Fig. 3 Debris flow intensity index (I_{DF}) against damage class. The bar graphs indicate the number of observations in each group to illustrate the group centroids. Different building classes are indicated by unique symbols

Once flow depth and flow velocity have been estimated or back-calculated for the different hazard scenarios to be considered, Table 4 can be applied to determine the probability for each damage class. For example, for $I_{DF} > 1000$ (Fig. 1), there is 100% chance that the impact will result in complete building destruction, whereas $I_{DF} < 1$ results in a 30% chance of some structural damage and 70% chance of only some sedimentation damage. For damage calculations in this example, one can either use the fractional likelihoods presented herein or, using conservative engineering principles, assume that all buildings will suffer some structural damage.

4 Application

Table 4 provides a way to apply the debris-flow intensity index (I_{DF}) to estimate a building's vulnerability. The key lies in estimating flow velocity and maximum flow depth within reasonable ranges. This can be accomplished by application of empirical or

Fig. 4 Sarno debris flows, damage class I–III. The estimated I_{DF} for the events shown on this photograph is 1–43. Photograph: http://pieffeeffe.files.wordpress.com/2008/05/sarno.jpg

numerical methods or expert judgment. In all cases, ranges should be presented to account for uncertainty. Average or maximum flow depth can be estimated from test trenches in which individual flows can clearly be discerned or by application of numerical methods. For defensible results, field-based studies should be used to calibrate the numerical models. Deposit depth may need to be adjusted for maximum flow depth by a factor that accounts for the assumed volumetric water content. Runup or superelevation of debris against rigid structures may need to be used to adjust flow depth, particularly if the obstacle is believed to create a back-water effect, thus increasing the depth of material deposited upstream of a building.

The following sections provide one test case (Sarno, Italy) that is part of the cases included in the database, and one predictive example where the scenario considered has not yet occurred and economic losses have not been determined (Mosquito Creek, Canada).

4.1 Sarno, Italy

Sarno is located in the Southern Campania Region of Italy at the foot of the Sarno Mountains. On 5–6 May 1998, the Sarno region experienced 9 large debris flows following 9 straight days of intense rainfall (Fig. 4). This incident resulted in 150 fatalities and extensive property damage in the towns of Sarno and Episcopio. Due to the serious consequences of this event, it was very well documented with respect to flow depths and flow velocities as well as the extent of damage experienced by the affected buildings. A modified version of the Damage Probability Model (Table 5) was created for this test. The modified probability model excludes all data from the Sarno case study to make the test more objective. Table 6 provides a comparison of the actual damage of buildings and the probability of damage predicted by a modified version of our model. The matrix assigns the highest probability to the observed damage class in half of all cases. For example, the modified probability matrix that predicted buildings located within the I_{DF} *isoéntasi* (line of same or similar intensity) of 5 (m^3/s^2) in debris flow event no. 8 corresponds to a 27% chance of damage class I, a 53% chance of damage class II, a 13% chance of damage class III and a 7% chance of damage class IV. Therefore, buildings affected by I_{DF} of 5 are most likely to be damaged as described by class II some structural damage, which matches the

Table 5 Damage class probabilities with Sarno case study data removed

Damage class probabilities given I_{DF} (%) WITHOUT SARNO DATA					
Complete destruction (IV)	0	7	33	67	100
Major structural damage (III)	0	13	25	28	0
Some structural damage (II)	17	53	42	5	0
Some sedimentation (I)	83	27	0	0	0
I_{DF}	0–1	$1–10^1$	$10^1–10^2$	$10^2–10^3$	$>10^3$

Table 6 Damage probabilities for the Sarno debris flow case study

Debris flow name	Avg. impact index (v^2h)	Number of concrete structures	Actual impact damage	Predicted probability of damage (%)			
				I	II	III	IV
Sarno debris flow 7	<1	16	Some sedimentation (I)	**83**	17	0	0
	1	7	Some structural (II)	27	**53**	13	7
	5	**22**	Major structural (III)	27	53	*13*	7
Sarno debris flow 8	<1	30	Some sedimentation (I)	**83**	17	0	0
	1	32	Some structural (II)	27	**53**	13	7
	5	15	Some structural (II)	27	**53**	13	7
	5	**10**	Major structural (III)	27	53	*13*	7
	14	3	Some structural (II)	0	**42**	25	33
	14	**7**	Major structural (III)	0	42	*25*	33
	26	**5**	Major structural (III)	0	42	*25*	33
	43	**1**	Major structural (III)	0	42	*25*	33

Bold fonts in the predicted probability column indicate where the observed and predicted damages match. Italic font indicates those damage classes where the predicted damage was still assigned a significant probability even though the observed damage differed from the predicted value

observed damage in 15 of 25 buildings. In those cases where the predicted damage class does not match the observed damage, the matrix still assigns a significant probability to the observed damage class. Given the uncertainties in predicting the exact velocity or flow depth, a perfect match cannot be expected and is unnecessary, since in most cases, the overall economic damage will be the study's objective rather than a precise building damage estimate.

4.2 Mosquito Creek, Canada

Mosquito Creek drains a 15.5-km^2 watershed in the District of North Vancouver (DNV), British Columbia. The DNV is located at the foot of the North Shore Mountains and receives, on average, approximately 2,400 mm of rainfall annually at lower elevations, with most of this falling during the period from November to February. Residential development of the DNV began in the late 1800s and proceeded rapidly through the 1950s to 1970s, including slopes adjacent to Mosquito Creek. After a major flood in the 1950s, it was decided to route a section of Mosquito Creek into a culvert with the aim to decrease flood hazard. Previous studies determined that the creek is subjected to debris floods

Table 7 Damage probabilities for Mosquito Creek and the total number of houses affected

Number of homes affected	Damage class			
	I	II	III	IV
	Probability of damage (%)			
21	70	30	0	0
13	22	50	22	6
3	0	37	38	25

(Kerr Wood Leidal, 2003), and debris flood characteristics for events ranging from 100- to 2500-year return periods have been more recently modelled based on input data from empirical methods, dendrochronology and some judgment (BGC Engineering Inc 2010). For return periods exceeding 100 years, the debris flood could overwhelm the intake of the culverted section and discharge through the former channel, impacting a densely developed area.

Table 7 summarizes the results for the 37 properties potentially affected for the 500-year debris flood.

Using the statistics derived from Table 4 and assuming that the event was a debris flow, two homes would be completely destroyed ($3 \times 0.25 + 13 \times 0.06$), 4 houses would suffer major structural damage ($13 \times 0.22 + 3 \times 0.38$), 14 houses would be affected by some structural damage ($3 \times 0.37 + 13 \times 0.50 + 21 \times 0.30$) and 18 houses would be affected by some sedimentation ($13 \times 0.22 + 21 \times 0.70$). At a nominal home value of CDN $ 1 million and using Table 4 as a guide to approximate monetary loss with the mean class values applied, this would result in a total loss of approximately CDN $ 14.3 million ($2 \times \$\ 1\ \text{M} + 4 \times \$\ 0.75\ \text{M} + 14 \times 0.5\ \text{M} + 18 \times 0.125\ \text{M}$).

This example serves to illustrate the method but does not replace a detailed economic analysis in which assessed or market values of each property are used and better data for percentage loss are obtained from insurance companies. Alternatively, where existing, the HAZUS model can determine total economic losses based on their database of property value and replacement costs. The principal limitation in this example is that the vulnerabilities applied were calibrated for debris flows, not debris floods, although some overlap is unavoidable since debris flows undergo phase changes during their descent. Nevertheless, the above estimates are likely conservative and could be adjusted for lower impact forces associated with debris floods, whose density may be half that of a debris flow. On the other hand, debris floods may be more erosive, leading to bank or channel erosion which could also result in damage. For economic risk assessments, therefore, the approach outlined above may be suitable for debris flows and debris floods alike.

5 Discussion

An exact prediction of building vulnerability to debris flow impact is not possible. This can be attributed principally to the uncertainty in estimating debris flow velocities and flow depths at the point of impact for different debris-flow scenarios. Furthermore, the exact elastic, plastic or rigid behaviour of buildings cannot be determined with great accuracy because the material types and their behaviour will usually not be known and will undergo changes due to ageing. Finally, debris flow impact will have dynamic and static impacts that are difficult to predict. Surges following the frontal lobe can pile up on top of the first

Fig. 5 Spring lake debris flow, damage class II. The estimated I_{DF} for this event is 5. Photograph: U.S. Forest Service

one and create loading conditions that may be difficult to forecast. These limitations suggest that a simple empirical approach to estimating building vulnerability from debris flow impact is desirable.

Error is also introduced in our assessment by limited accuracy of reported velocities and maximum flow depths. While the latter can be readily measured (if the building's base elevation is known or can be excavated), the former is hardly ever measured directly. This means that velocities must be back-calculated or estimated from eye witness accounts. Consequently, every reported value will have considerable error.

A differentiation between building type is represented by assigning unique symbols to each building class (Fig. 3), but this could not identify a unique relationship for each building class due to the small sample size and low precision level of damage in the database. The majority (44%) of the buildings consisted of standard wood frame construction (Fig. 5), 20% consisted of masonry construction, 12% consisted of poorly constructed villages in developing countries, 10% consisted of infrastructure structures and 4% of structures could not be categorized because of insufficient data.

Most events discussed in the literature pertain to catastrophic occurrences which lend themselves to scientific investigation and publication. However, this may create some bias towards the upper spectrum in impact forces and thus I_{DF}. An open database that would also benefit from consulting reports of minor incidences could, over time, minimize this bias.

6 Conclusion

Quantitative debris flow risk assessments increasingly form the basis for making decisions on the need for, and scale of, engineered mitigation measures versus land use decisions. Within the risk evaluation phase, target or tolerable risks are defined by the local or higher levels of government which, when exceeded, may be reduced through land use planning or engineered structures until the residual risk is deemed tolerable or acceptable.

Quantitative risk assessment methodology has been well established, but its accuracy hinges on the accuracy of its input parameters. With the application of appropriate methods, P_H, $P_{S:H}$, $P_{T:H}$ and E (for loss of life risk) can be estimated with reasonable confidence. Where such confidence cannot be achieved, error bands should be reported and be integrated in the risk calculations. Vulnerability of buildings from debris-flow impact may be the least quantifiable variable, which is unfortunate because it also relates directly to human vulnerability since debris flows kill people mostly by damaging or destroying their dwellings.

A global literature review yielded 68 case studies for which debris flow intensity and damage were known or could be estimated with the data presented. Four damage classes were defined ranging from minor sedimentation to complete building destruction. We did not differentiate as to building type as such differentiation would have reduced the total sample size to an extent where the number of cases in each damage class would be too low for a robust probabilistic assessment. A debris flow intensity index (I_{DF}) was created by multiplying flow depth and the square of flow velocity. The I_{DF} best differentiates between the four damage classes and is also physically meaningful because it surrogates impact force.

The method was demonstrated on Mosquito Creek where an event has not occurred but where flow depths and flow velocities have been estimated through numerical modelling. The estimated total damage for a 500-year event was determined to be approximately CDN $ 14 M in 2011 dollars. The method was further tested for the very well-documented Sarno debris flows. In this case, the monetary loss was ignored and the comparison between predictions and observations focused on the damage classes. In half of all cases, the highest predicted probability for the associated damage class matched the observed damage. For the other cases, a significant probability was associated with the observed damage class.

Using the assessed or estimated building value and information provided by insurance underwriters or home builders on replacement costs, the economic loss can be calculated for each home and summed for all houses for each of the event scenarios considered. All of these data, along with the damage functions, could be input and modelled within HAZUS to come up with the damage and loss scenarios for each event which can include building damage, economic losses, casualties, displaced households and shelter requirements.

In most jurisdictions, economic risk tolerance criteria do not exist, but standard benefit-cost analyses (BCA) may be used to determine the necessity, scale and cost of engineered risk reduction measures and weigh them against land use changes. Such an approach is useful but cannot replace a multi-criteria assessment (MCA) where the potential of loss of life is integrated as a minimum. Other factors such as political damage (the legal and public relations repercussions if nothing, or not enough, had been done to prevent damage), human suffering due to injury or loss of loved ones, environmental losses due to destruction of sensitive habitat or pollution of water courses by hazardous substances could all be integrated in such MCA. This study was designed to provide a convenient and repeatable method to estimate the likely building damage and their direct economic losses due to debris flow impact.

The database created as part of this project can be enlarged by many case studies that were not found during the literature search or can only be found in the grey literature. The database will be made public and accessible, and we encourage other researchers to add their own case studies in the database in a wiki-type process for further improvement. This open-source process will later allow stratifying the data set into different building types or allow the development of improved impact indices and correlations.

Acknowledgments This work was made possible and supported by the Chemical, Biological, Radiological/Nuclear, and Explosives Research and Technology Initiative (CRTI) and the Public Security Technical Program (PSTP)—(Quantitative Risk Assessment Project 09/10-0001SCP), which is managed by the Defence Research and Development Canada—Centre for Security Science and Natural Resources Canada. Comments by Murray Journeay, Nicky Hastings, Rejean Couture, Scott McDougall and two anonymous reviewers are acknowledged.

References

Aleotti P, Polloni G (2003) Two-dimensional model of the 1998 Sarno debris flows (Italy): preliminary results. Debris-flow hazards mitigation: mechanics, prediction, and assessment; 2003 ISBN 90 77017 78 X

Armanini A (1997) On the dynamic impact of debris flows. Recent developments on debris flows. Lecture Notes in Earth Sciences, 64. Springer, Berlin

Beaupre MM (2009) Structural damage due to the impact pressure generated by the 2005 Berkeley debris slide, located in North Vancouver, B.C. UBC B.A.Sc. Thesis

BGC Engineering Inc. (2003) Preliminary debris flow hazard assessment Hatzic valley. Provincial emergency program. Prepared for the Ministry of Environment. ftp://ftp.for.gov.bc.ca/DCK/external/%21publish/Stewardship/Hydrology_Terrain%20Stability/Hatzic/Reports/BGC%20Engineering%20Hatzic%20Valley%20Report%202003.pdf

BGC Engineering Inc (2010) Mosquito Creek debris flow flood: quantitative risk and mitigation option assessment. District of North Vancouver. Accessed via http://www.dnv.org

Blais-Stevens A, Septer, D (2008) Historical accounts of landslides and flooding events along the Sea to Sky Corridor, British Columbia, from 1855–2007. Geological Survey of Canada 48–49 pp. 62–68 pp. 71–73 pp

Borter P (1999) Risikoanalyse bei gravitativen Naturgefahren, Bundesamt für Umwelt. Wald und Landschaft, Bern, p 1999

Bovis MJ, Dagg BR (1992) Debris flow triggering by impulsive loading: mechanical modelling and case studies. Can Geotech J 29:345–352

Catane SG, Cabria HB, Tomarong CP Jr, Saturay RM Jr, Zarco MA, Pioquinto WC (2007) Catastrophic Rockslide-debris avalanche at St. Bernard, Southern Leyte, Philippines. J Int Consort Landslides 4(1):85–90

Chen JH, Lee CF (2007) Landslide mobility analysis using Modflow. The 2007 international forum on landslide disaster management; ISBN 978-962-7619-30-7

Chen NS, Li TC, Gao YC (2005a) A great disastrous debris flow on 11 July 2003 in Shuikazi Valley, Danba County, Western Sichuan, China. Landslides 2:71–74

Chen N, Li T, Gao Y (2005b) A great disastrous debris flow on 11 July 2003 in Shuikazi Valley, Danba County, Western Sichuan, China. J Int Consort Landslides 2(1):71–74

Chou HT, Liao WM, Lin ML (2000) Landslide induced debris-flow at a dump site. Debris-flow hazards mitigation: mechanics, prediction, and assessment; 2000. ISBN 90 5809 149 X

Chow VT (1959) Open channel hydraulics. McGraw hill, New York 680 p

Conedera M, Peter L, Marxer P, Forster F, Rickenmann D, Re L (2003) Consequences of forest fires on the hydrogeological response of mountain catchments: a case study of the Riale Buffaga, Ticino, Switzerland. Earth Surf Proc Land 28:117–129

Evans SG, Bishop N, Smoll LF, Murillo PV, Delaney KB, Oliver-Smith A (2009) A re-examination of the mechanism and human impact of catastrophic mass flows originating on Nevado Huascaran, Cordillera Blanca, Peru in 1962 and 1970. Eng Geol 108:96–118

Fell R, Hartford D (1997) Landslide risk management. In: Cruden D, Fell R (eds) Landslide risk assessment. Balkema, Rotterdam, pp 51–109

FEMA (Federal Emergency Management Agency) (2003) www.fema.gov/plan/prevent/Hazus/index.shtm

Fuchs S, Heiss K, Hübl J (2007) Towards an empirical vulnerability function for use in debris flow risk assessment. Nat Hazards Earth Syst Sci 7:495–506

Garcia-Martinez R, Lopez JL (2005) Debris flow of December 1999 in Venezuela. In: Jakob M, Hungr O (eds) Debris-flow hazards and related phenomena. Praxis. Springer, Berlin 519 pp

Haeberli W, Huggel C, Kaa A, Zgraggen-Oswald S, Polkvoj A, Galushkin I, Zotikov I, Osokin N (2004) The Kolka-Karmadon Rock/Ice Slide of 20 September 2002: an extraordinary event of historical dimensions in North Ossetia, Russian Caucasus. J Glaciol 50(171):533–546

Hancox GT (2003) Preliminary report on landslides, gully erosion, and debris flood effects in the Pae-kakariki area as a result of the 3 October 2003 flood. Institute of Geological and Nuclear Sciences Limited. Institute of Geological and Nuclear Sciences client report 2003/120. Project No. 430W1094. 19 pp. http://geonet.org.nz/content/download/7524/44019/file/report4.pdf

Haugen ED, Kaynia AM (2008) Vulnerability of structures impacted by debris flow. Landslides and Engineered Slopes—Chen et al. (eds), pp 381–387

Hsu SM, Chiou LB, Lin GF, Chao CH, Wen HY, Ku CY (2010) Applications of simulation technique on debris flow hazard zone delineation: a case study in Hualien County, Taiwan. Nat Hazards Earth Syst Sci 10:535–545

Hübl J, Holzinger G (2003) Kleinmassstäbliche Modellversuche zur Wirkung von Murbrechern, WLS Report 50, Band 3, Universität für Bodenkultur, Wien

Hungr O, Morgan GC, Kellerhals R (1984) Quantitative analysis of debris torrent hazards for design of remedial measures. Can Geotech J 21:663–677

Jakob M (2005) A size classification for debris flows. Eng Geol 79:151–161

Jakob M, Anderson D, Fuller T, Hungr O, Ayotte D (2000) An unusually large debris flow at Hummingbird Creek, Mara Lake, British Columbia. Can Geotech J 37:1109–1125

Kherkheulidze II (1976) Estimation of basic characteristics of mud flows ("sels"). In: Proceedings of the Leningrad symposium august 1967, international association of scientific hydrology (IAHS) studies and reports in hydrology, No. 3, Vol. 2, pp 940–948

Kong J, Chen Z, Song S (2006) Occurrence conditions and process analysis on fluidization of valley type landslide: example of the fluidization of landslide in Qiongshan Ravine, Danba. Wuhan Univ J Nat Sci 11(4):829–834

McDougall S, Boultbee N, Hungr O, Stead D, Schwab JW (2006) The Zymoetz River landslide and dynamic analysis of a rock slide-debris flow. J Int Consort Landslides 3(3):195–204

McSaveney MJ, Davies TRH (2005) Engineering for debris flows in New Zealand. In: Jakob M, Hungr O (eds) Debris-flow hazards and related phenomena. Praxis. Springer, Berlin 651 pp

Medina V, Hürlimann M, Bateman A (2008) Applications of FLATModel, a 2D finite volume code, to debris flows in the Northeastern Part of the Iberian Peninsula. J Int Consort Lands 5(1):127–142

Mueller R, Loew S (2009) Predisposition and cause of the catastrophic landslides of August 2005 in Brienz (Switzerland). Swiss J Geosci 1–14

Nakagawa H, Takahashi T, and Satofuka Y (2000) A debris-flow disaster on the fan of the Harihara River, Japan. Debris-flow hazards mitigation: mechanics, prediction, and assessment; 2000. ISBN 90 5809 149 X

Ni H, Zheng W, Li Z, Ba R (2010) Recent catastrophic debris flows in Ludig County: geological hazards, rainfall analysis, and dynamic characteristics. Nat Hazards 55:523–542

Rapp A, Li J, Nyberg R (1991) Mudflow disaster in mountainous areas. Ambio 20(6):210–218

Revellino P, Hungr O, Guadagno FM, Evans SG (2004) Velocity and runout simulation of destructive debris flows and debris avalanches in pyroclastic deposits, Campania Region, Italy. Env Geol 45:295–311

Rickenmann D (1999) Empirical relationships for debris flows. Nat Hazards 19:47–77

Scott KM (2000) Precipitation-triggered debris-flow at Casita Volcano, Nicaragua: implications for mitigation strategies in Volcanic and tectonically active Steeplands. Debris-flow hazards mitigation: mechanics, prediction, and assessment; 2000. ISBN 90 5809 149 X

Suwa H (2003) Repetition of debris flows on sunny days at a torrent in Karakorum. Debris-flow hazards mitigation: mechanics, prediction, and assessment; 2003. ISBN 90 77017 78 X

Suwa H, Nakaya S (2007) Two catastrophic debris avalanches triggered by rainstorms in Japan and Philippines. In: Debris-flow hazards mitigation: mechanics, prediction, and assessment, Chen and Major, eds; 341–351 pp

Suwa H, Yamakoshi T (2000) Estimation of debris-flow motion by field surveys. debris-flow hazards mitigation: mechanics, prediction, and assessment; 2000. ISBN 90 5809 149 X

Thurber Consultants Ltd (1983) Debris torrent and flooding hazards: Highway 99, Howe Sound. Prepared for Ministry of Transportation. April 1983

Totschnig R, Sedlacek W, Fuchs S (2011) A quantitative vulnerability function for fluvial sediment transport. Nat Hazards 58(2):681–703

Toyos G, Oppenheimer C, Pareschi MT, Sulpizo R, Zanchetta G, Zuccaro G (2003) Building damage by debris flows in the Sarno Area, Southern Italy. Debris-flow hazards mitigation: mechanics, prediction, and assessment; 2003. ISBN 90 77017 78 X

Tropeano D, Turconi L, Rosso M, Cavallo C (2003) The October 15, 2000 Debris Flow in the Bioley Torrent, Fenis, Aosta Valley, Italy—Damage and Processes. Debris-Flow Hazards Mitigation: Mechanics, Prediction, and Assessment; 2003. ISBN 90 77017 78 X

Utah Geological Survey (2002) September 12, 2002, Fire-related debris flows East of Santaquin and Spring Lake. Utah County, Utah

VanDine DF, Rodman RF, Jordan P, Dupas J (2005) Kuskonook Creek, an example of a debris flow analysis. J Int Consort Landslides 2(4):257–265

Wang CX, Esaki T, Li S (2008) GIS-based two-dimensional numerical simulation of rainfall-induced debris flow. Nat Hazards Earth Syst Sci 8:47–58

Wigmosta MS (1983) Rheology and flow dynamics of the Toutle debris flows from Mt. St. Helens. M.Sc. thesis, University of Washington, Seattle, pp 184

Xu Q, Fan X, Huang R, Yin Y, Hou S, Dong X, Tang M (2010) A catastrophic rockslide-debris flow in Wulong, Chongqing, China in 2009: background, characterization, and causes. Landslides 7:75–87

Zanchetta G, Sulpizo R, Pareschi MT, Leoni FM, Santacroce R (2004) Characteristics of May 5–6, 1998 volcaniclastic debris flows in the Sarno Area (Campania, southern Italy): relationships to structural damage and hazard zonation. J Volcanol Geotherm Res 133:377–393

Zimmermann MN (2005) Analysis and management of debris-flow risks at Sorenberg (Switzerland). In: Jakob M, Hungr O (eds) Debris flow hazards and related phenomena. Praxis. Springer, Berlin